BULLETIN OF THE POLISH ACADEMY OF SCIENCES
TECHNICAL SCIENCES, Vol. 69(5), 2021, Article number: e137416
DOI: 10.24425/bpasts.2021.137416

High temperature resistance of silicide-coated niobium

Radosław SZKLAREK[1, 2, 3], Tomasz TAŃSKI[1], Bogusław MENDALA[1], Marcin STASZUK[1], Łukasz KRZEMIŃSKI[1], Paweł NUCKOWSKI[1], and Kamil SOBCZAK[3]

[1] Silesian University of Technology, ul. Akademicka 2A, 44-100 Gliwice, Poland
[2] Spinex Spinkiewicz Company, Klimontowska 19, 04-672 Warsaw, Poland
[3] Łukasiewicz Research Network – Institute of Aviation, al. Krakowska 110/114, 02-256 Warsaw, Poland

Abstract. In this paper, thermal oxidation resistance of silicide-coated niobium substrates was tested in a temperature range of 1300–1450°C using an HVOF burner. Pure niobium specimens were coated using the pack cementation CVD method. Three different silicide thickness coatings were deposited. Thermal oxidation resistance of the coated niobium substrates was tested in a temperature range of 1300–1450°C using an HVOF burner. All samples that passed the test showed their ability to stabilize the temperature over a time of 30 s during the thermal test. The rise time of substrate temperature takes about 10 s, following which it keeps constant values. In order to assess the quality of the Nb-Si coatings before and after the thermal test, light microscopy, scanning electron microscopy (SEM) along with chemical analysis (EDS), X-ray diffraction XRD and Vickers hardness test investigation were performed. Results confirmed the presence of substrate Nb compounds as well as Si addition. The oxygen compounds are a result of high temperature intense oxidizing environment that causes the generation of SiO phase in the form of quartz and cristobalite during thermal testing. Except for one specimen, all substrate surfaces pass the high temperature oxidation test with no damages.

Key words: niobium; silicide; thermal barrier coating; CVD; high temperature oxidation resistance.

1. INTRODUCTION

Niobium and its alloys are used for high temperature applications in the aerospace and space industry [1–3]. Their high melting point allows these materials to be used in the construction of jet engine chambers and turbine blades. However, niobium is not resistant to high temperature oxidation. It is oxidized at over 350°C and needs surface protection against material degradation [4–7]. Various techniques may be used for refractory metals coating, including APS, HVOF, laser alloying, PVD (arc sputtering) and CVD (pack cementation). All of these techniques can create thermal barrier coatings (TBC) of thickness in the range of hundreds of microns, with a characteristic thermal growing oxides (TGO) area [8–11]. One of more effective anti-oxidation protection methods involves aluminides and silicides based coatings [12]. For example, the Nb_5Si_3 phase is stable for up to 1765°C and reacts with oxygen during high temperature oxidation, creating silicide oxides on top of the coating [13]. It acts as a passive layer which protects coating against oxygen diffusion. Silicides constitute a good high temperature protection choice for niobium and its alloys due to their outstanding resistance to high-temperature oxidation, uncomplicated preparation method, good ability to self-heal and strong bonding with the niobium alloy. The oxidation resistance of silicides depends on their crystallographic structure and chemical stechiometry. Among niobium silicides, Nb_7Si_6 has the greatest oxidation resistance because of high potential in its structure modification. This ability allows to dope the Nb_7Si_6 structure with various elements. This method has been performed and tested in the last decades in order to improve oxidation resistance [1, 14–17].

There are known other publications [18–26] which are focused on silicide coatings and investigate their influence on high oxidation resistance of various materials such as niobium, molybdenum and titanium alloys.

The purpose of this work was to prepare niobium silicide coatings on the surfaces of pure niobium using the CVD technique to form a protective SiO2 coating layer at elevated temperatures. The structure and properties of the coating were investigated along with oxidation resistance during exposure of silicide-coated niobium at 1400°C, using an HVOF burner.

2. EXPERIMENT

Pure niobium (99.95%) substrates in the form of discs with diameter of 50 mm and thickness of 3 mm were grinded to a 1200-grade finish using SiC abrasive papers applied with STRUERS Tegramin-30. Cleaned specimens were coated with silicides using the pack cementation CVD method. Three different thicknesses of NbSi coating were created as 50 µm (marked as W1), 70 µm (W2) and 90 µm (W3). Coated samples were cut for cross section microscopy analysis, grinded up to a 2500-grade finish using SiC abrasive papers and polished with OPU liquid.

*e-mail: radoslaw.szklarek@gmail.com

Manuscript submitted 2021-03-01, revised 2021-04-07, initially accepted for publication 2021-04-12, published in October 2021

Oxidation behavior of the coated specimens was examined at 1400°C for 30 s using an HVOF flame burner.

Such a high temperature was chosen because of potential application where a temperature of 1400°C and a high oxidation process have a destructive influence over niobium during even half a minute.

Both coated and oxidized specimens were analyzed to determine the phase composition of the substrate and silicides coating. X-ray diffraction tests were performed. For this purpose, an X'Pert Pro MPD X-ray diffractometer by Panalytical, equipped with a copper lamp ($\lambda K\alpha = 0.154$ nm) and a semiconductor detector on the bent beam axis, was used. Diffraction lines were recorded in Bragg-Brentano geometry in the angular range of 10–120° [2θ] with a 0.05° step and the time of 50 s per step. Analysis of the obtained diffractograms was performed using the Panalytical High Score Plus software, which contains a dedicated database of PAN-ICSD phase identification files. Scanning electron microscopy (SEM) and chemical analysis (EDS) investigation was performed using ZEISS – SUPRA 35 and EDAX – TRIDENT XM4. The FUTURE-TECH FM-ARS 9000 hardness tester was used for hardness testing at Vickers scale of HV0.05. Optical microscopy used the ZEISS – Xio Observer.

Pure and coated Nb samples were subjected to thermal testing using an HVOF flame in a fixed process parameter. The purpose of the test was to pre-determine the suitability of the produced coatings for use in high temperature applications. In addition, temperature was measured on the opposite side of the sample relative to the flame, in order to determine the thermal resistance of the coatings deposited on Nb substrates. The course of the thermal resistance test consisted of the following steps (Fig. 1):

1. Clamping a cylindrical sample with a diameter of 50 mm in the holder (tools steel) under 45° to the flame axis.
2. HVOF ignition and stabilization of combustion conditions away from the sample.
3. Rapid approach of the HVOF gun to the central position of the sample at the distance of 80 mm between the nozzle exit and the sample surface.
4. Holding for 30 s and simultaneous temperature measurement on the other side of the sample.
5. Quick nozzle departure, flame extinguishing and slow cooling of the sample in the air flow.

Another test was performed for high temperature oxidation resistance of silicide-coated niobium and the same process parameters were used.

Fig. 1. Thermal test of Nb sample without coating

6. RESULTS AND DISCUSSION

The NbSi coatings 50 μm, 70 μm and 90 μm in thickness were deposited on niobium samples.

Optical metalography was then performed for the W1, W2 and W3 samples.

Analyzing the coating structure, as shown in Fig. 2–4, allowed for characteristic columnar shape to be observed. This shape is a result of crystal-growing during the CVD process. It seems that there is relation between NbSi crystals size and the coating thickness. The smallest crystals grew in the W1 speci-

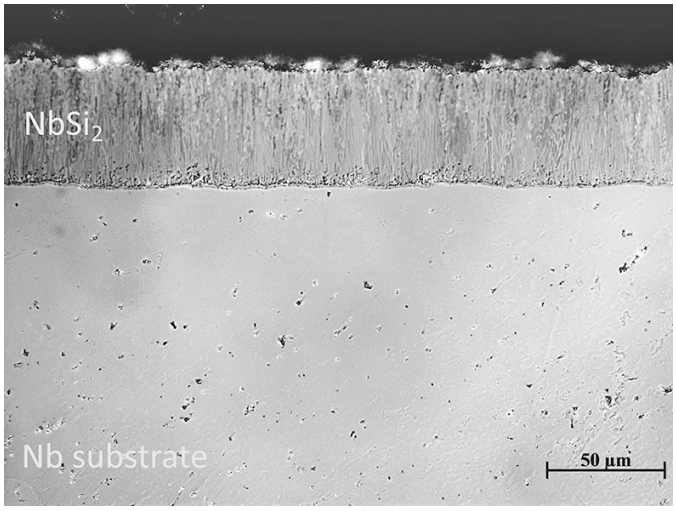

Fig. 2. Cross section of W1 sample. Columnar structure of NbSi coating can be observed on the top. Magnification ×500

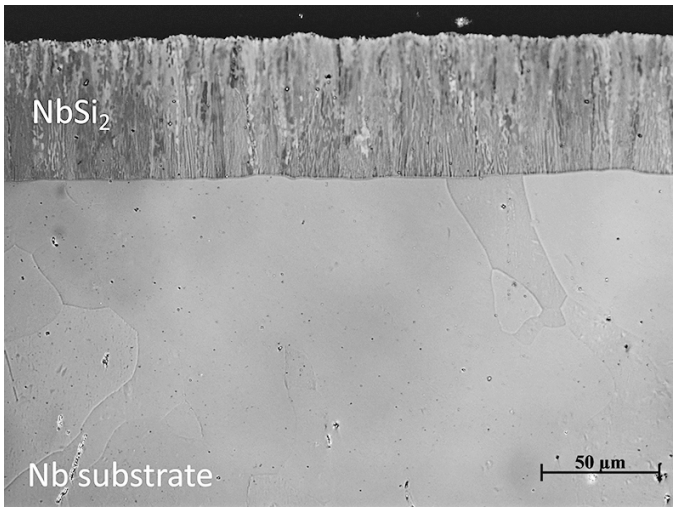

Fig. 3. Cross section of W2 sample. Columnar structure of NbSi coating can be observed on the top. Magnification ×500

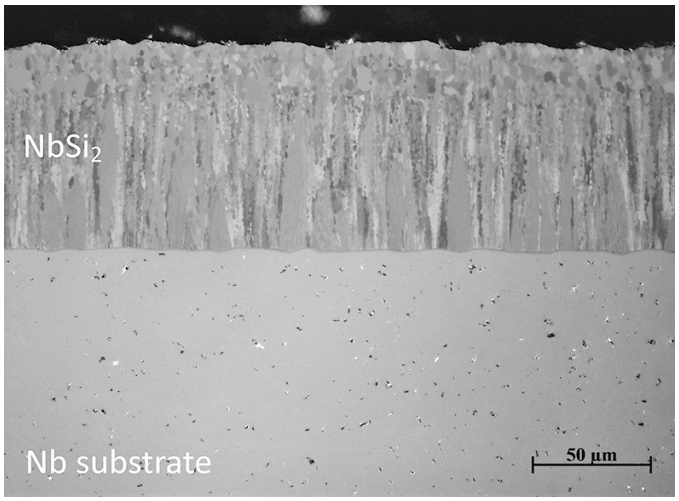

Fig. 4. Cross section of W3 sample. Columnar structure of NbSi coating can be observed on the top. Magnification ×500

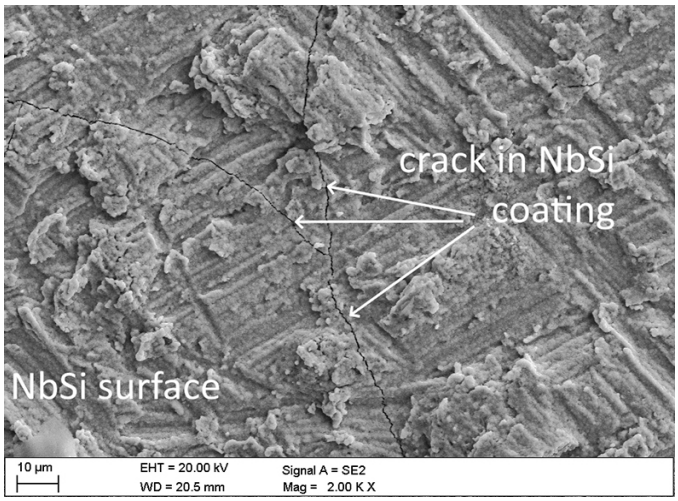

Fig. 6. SEM surface morphology of NbSi layer (W1 specimen). Cracks were observed on the NbSi surface

men and the largest ones – in W3. The coating of sample W1 is the thinnest (50 µm) and the CVD process time is shorter than for W2 and W3 samples, which have better thermal conditions for crystals growing.

Scanning electron microscopy cross section of the W3 specimen is shown in Fig. 5 and topography of W1–W3 is presented in Fig. 6–11. The NbSi coating is homogenous and a thin bond coat layer on the substrate surface is observed. This layer also has a columnar structure and may influence the coating structure above.

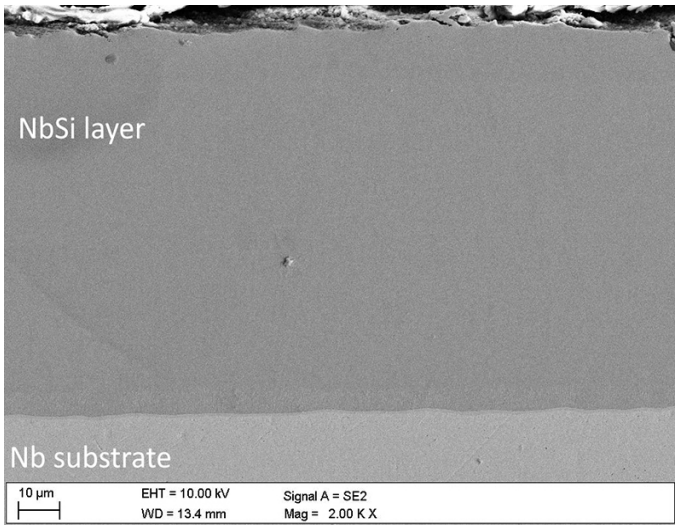

Fig. 5. SEM cross section of W3 sample. The NbSi layer visible as dark gray area

The coating surface topography it is not homogenous. Characteristic relief was observed as well as small cracks on the top. The cracks size relates to the specimen type. The smallest width of cracks occurred for sample W2.

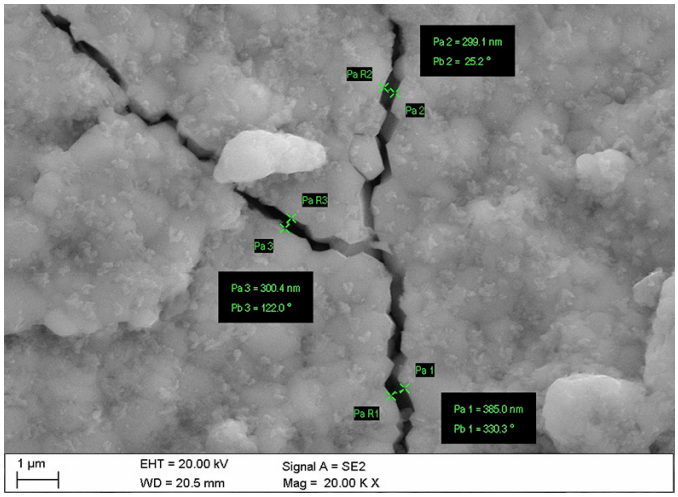

Fig. 7. Surface morphology of NbSi layer (W1 specimen). Cracks were observed on the NbSi surface

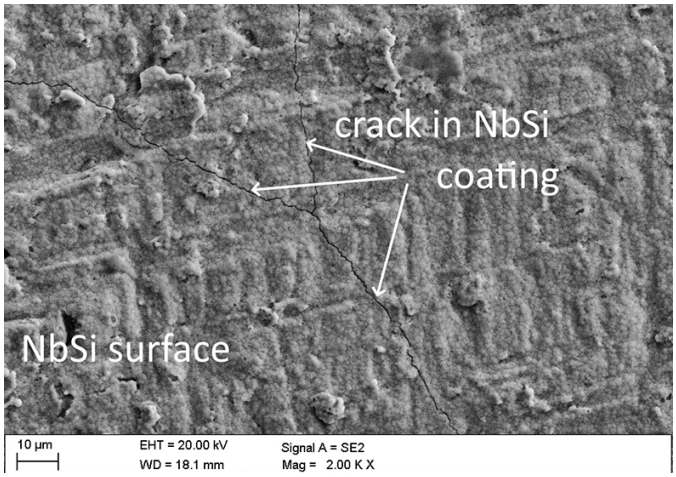

Fig. 8. Surface morphology of NbSi layer (W2 specimen). Cracks were observed on the NbSi surface

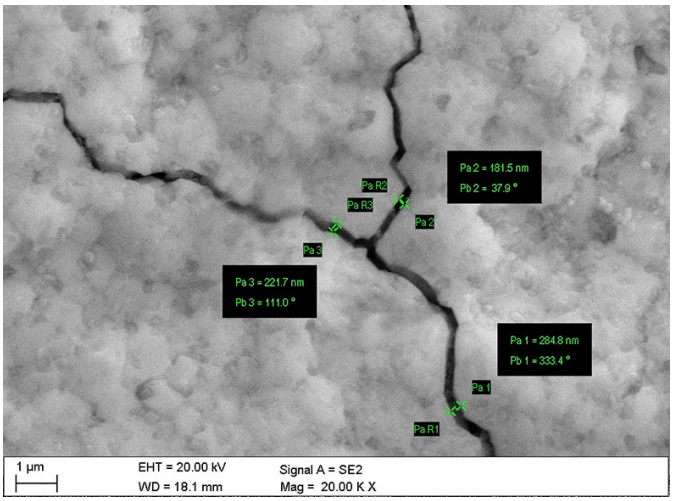

Fig. 9. Surface morphology of NbSi layer (W2 specimen). Cracks were observed on the NbSi surface

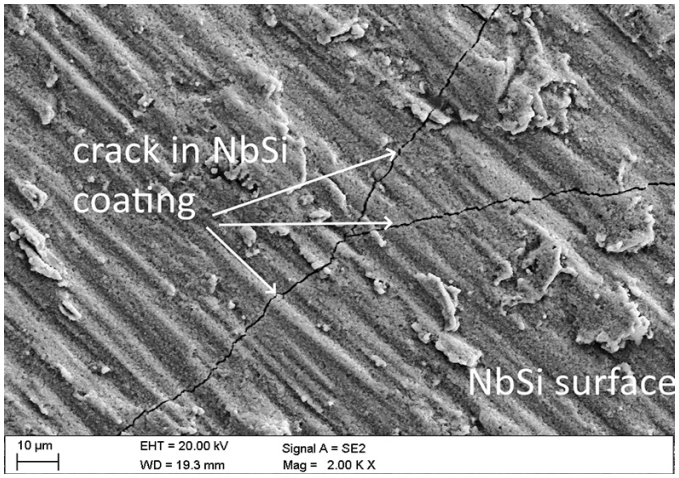

Fig. 10. Surface morphology of NbSi layer (W3 specimen). Cracks were observed on the NbSi surface

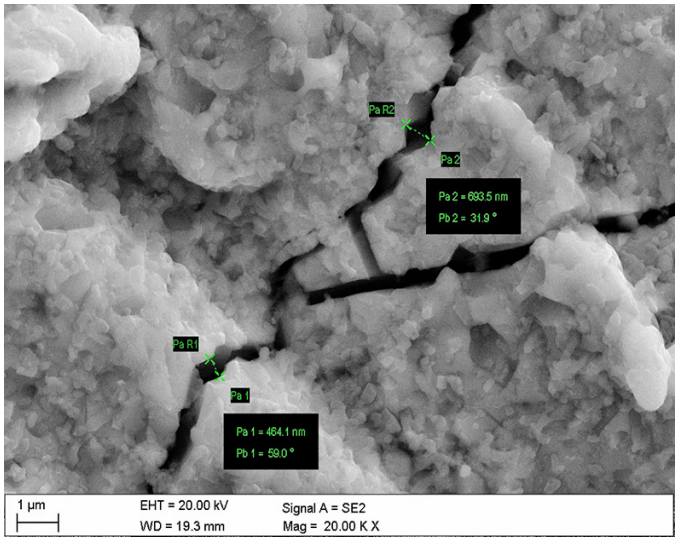

Fig. 11. Surface morphology of NbSi layer (W3 specimen). Cracks were observed on the NbSi surface

The coating surface EDS chemical analysis confirmed similar composition for all coated specimens which are shown in Fig. 6, 8 and 10 (Table 1–3).

Table 1
Chemical composition of 50 µm NbSi coating (W1)

Element	At%
Si	68.90
Nb	31.10

Table 2
Chemical composition of 70 µm NbSi coating (W2)

Element	At%
Si	69.90
Nb	30.10

Table 3
Chemical composition of 90 µm NbSi coating (W3)

Element	At%
Si	70.62
Nb	29.38

When analyzing Tables 1–3, the silicon At% content is observed to be more than twice as large as that of niobium. This could suggest that the created phases of silicide niobium are $NbSi_2$. It should be confirmed by XRD investigation.

According to the assumptions, the phases occurring in the substrates are in the case of a niobium substrate the phase with a predominant volume share is the Nb phase of a body-centered cubic network, space group Im-3m (ICSD: 98–064–5060) and in a lower proportion the Nb phase of a face-centered cubic structure, space group Fm-3m (ICSD: 98–004–1512) (Fig. 12). All specimens (W1, W2 and W3) revealed the presence of NbSi2 phases of hexagonal structure P 62 2 2 (ICSD: 90–060–1659) (Fig. 13–15).

The cross section hardness test was performed for W1, W2 and W3 specimens, including the substrate material (Table 4). The coatings hardness is constant for all thickness ranges from substrate surface to the coating top. There is a very high hard-

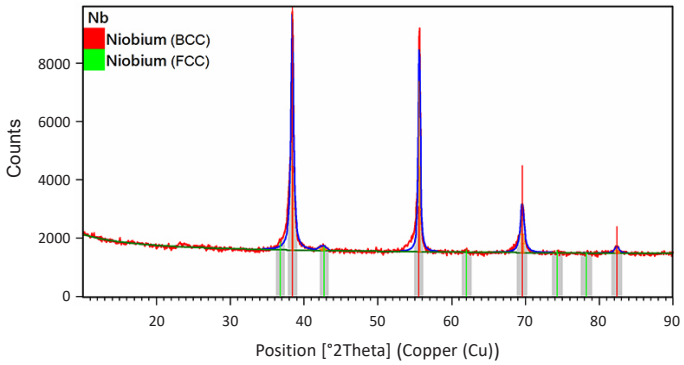

Fig. 12. X-ray diffraction pattern of Nb substrate

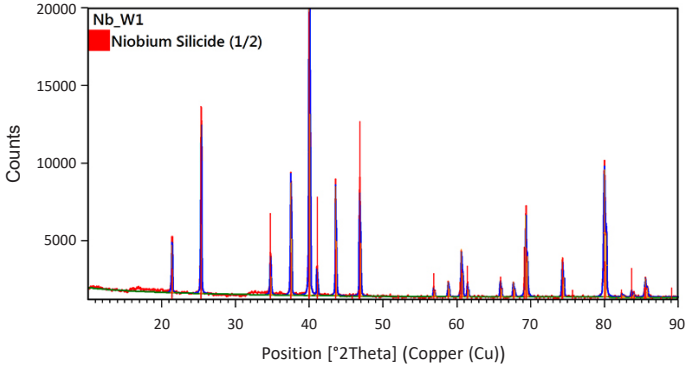

Fig. 13. X-ray diffraction pattern of silicon coatings on an Nb substrate, variant 1 (NbSi-W1)

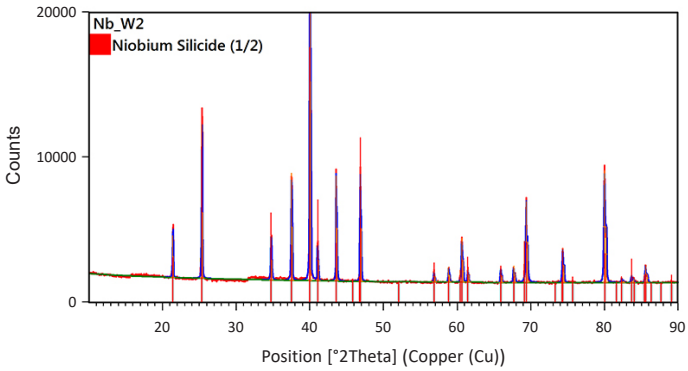

Fig. 14. X-ray diffraction pattern of silicon coatings on an Nb substrate, variant 2 (NbSi-W2)

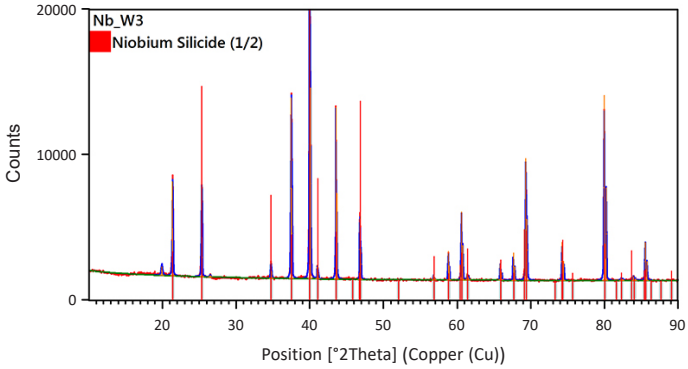

Fig. 15. X-ray diffraction pattern of silicon coatings on an Nb substrate, variant 3 (NbSi-W3)

Table 4
Hardness measurements of tested niobium samples

Specimen (Nb + NbSi)	Substrate hardness (Nb) [HV0.05]	Coating hardness (NbSi) [HV0.05]
W1 (NbSi 50 µm)	86	1,180
W2 (NbSi 70 µm)	83	1,180
W3 (NbSi 90 µm)	82	1,180

ness gradient between the substrate and coating, which may generate additional stress in the bond coat area and the coating structure. It has a negative influence on coating adhesion and its mechanical properties.

3. HIGH TEMPERATURE OXIDATION TEST

As a result of the HVOF heat test of samples not coated with TBC coating, a significant sparkle sputtering phenomenon was visible. The high velocity of gases as well as high temperature on the substrate surface causes materials sputtering. This thermal abrasive wear caused a form of a crater to occur and thinned the Nb sample (Fig. 16).

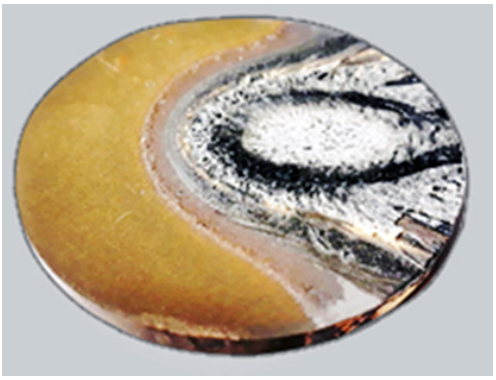

Fig. 16. Pure niobium substrate after thermal test (30 s). Magnification ×1. Material sputtering effect occurred. Yellow oxides on the surface were observed

As a result of the thermal test of Nb-NbSi TBC samples, the traces of wear were observed and rated. All of the samples, except for Nb-NbSi W2 (Fig. 18), passed the thermal test without significant destruction of the TBC layer or the metallic Nb substrate (Fig. 17, 19).

In order to assess the quality of the Nb-Si coatings after the thermal test, scanning electron microscopy (SEM) and chemi-

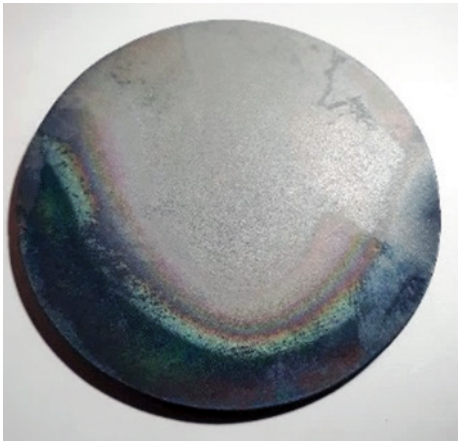

Fig. 17. W1 sample after high temperature oxidation thermal test. Magnification ×1. No material sputtering effect occurred

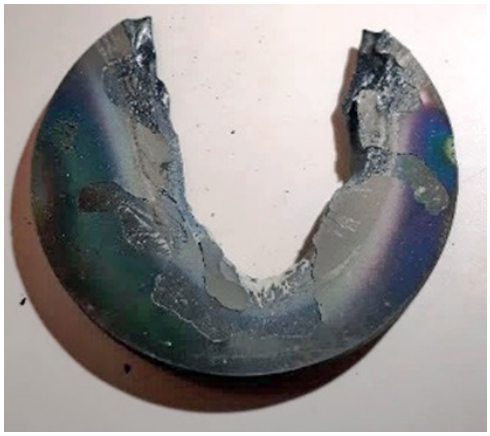

Fig. 18. W2 sample after high temperature oxidation thermal test (failed). Critical material sputtering process occurred. The specimen was destroyed. Magnification ×1

Fig. 19. W3 sample after high temperature oxidation thermal test. Magnification ×1. No material sputtering effect occurred

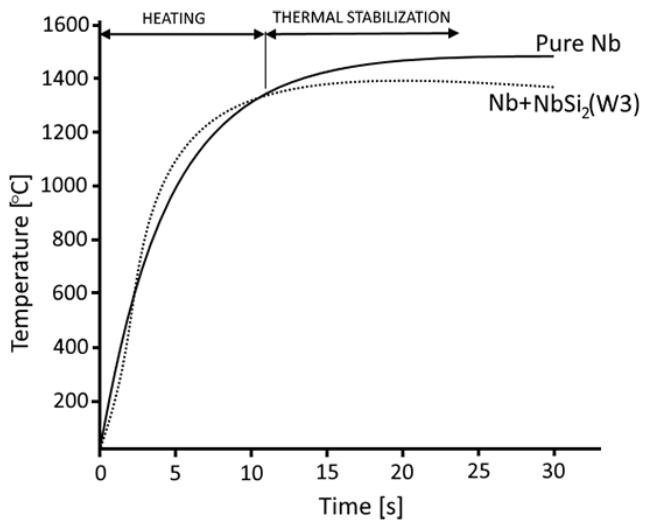

Fig. 20. Heating rate characteristic during thermal test of W3 sample (NbSi thickness – 90 µm) and pure niobium

Table 5
Surface chemical composition of NbSi coating (W3) after HVOF high temperature oxidation thermal test

Element	At%
Si	42.36
Nb	5.59
O	52.05

cal analysis (EDS) investigation were performed (Figs. 21–23, Table 5). Results confirmed the presence of substrate Nb compounds as well as Si addition. The oxygen compounds may be a result of the highly oxidizing environment that causes the generation of a SiO phase in the form of quartz and cristob-

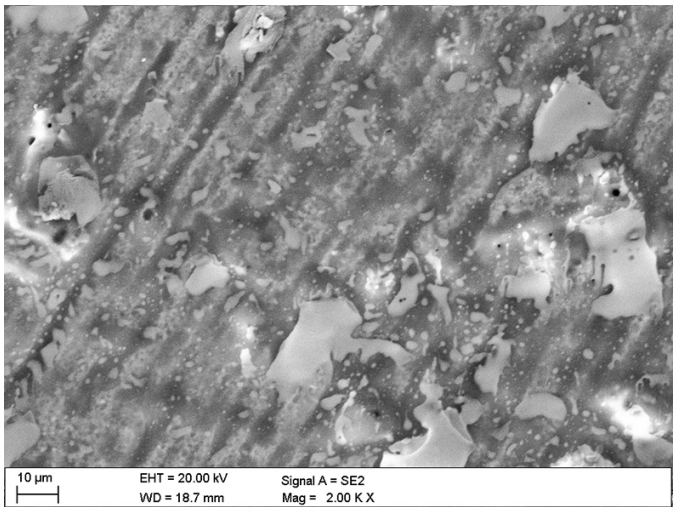

Fig. 21. NbSi topography after HVOF high temperature oxidation thermal test (W3 sample)

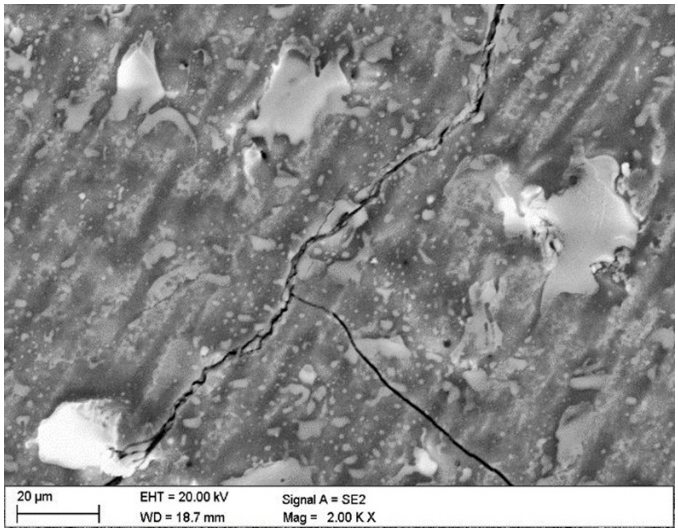

Fig. 22. NbSi topography after HVOF high temperature oxidation thermal test (W3 sample)

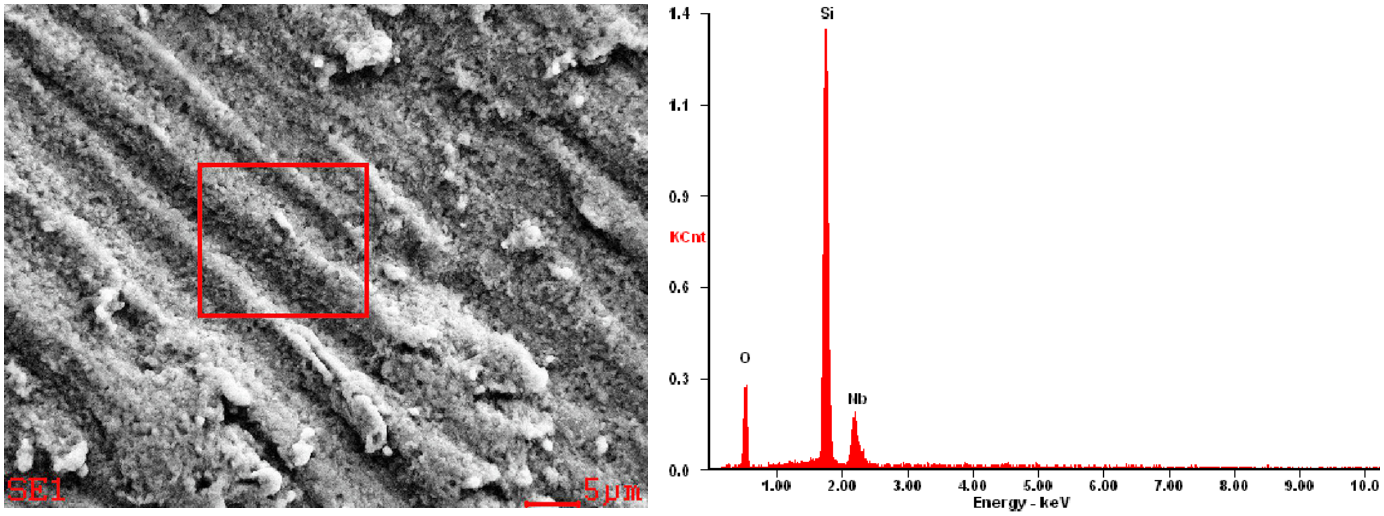

Fig. 23. Surface EDS chemical analysis in the defined area of NbSi coating (W3 sample) after HVOF high temperature oxidation thermal test

Table 6
Comparison of cracks width for various specimens

Specimen	Cracks width [nm]
W1	300–385
W2	180–280
W3	460–690
W3 (after thermal test)	1,000–1,500

alite during the thermal test. The SEM photography additionally shows some micro-cracks on NbSi TBC coating, which were also observed before thermal testing (Figs. 6–11). This may be a result of the influence of growing NbSi crystals at high temperature and thermal stress during the CVD process. Fortunately, the micro-cracks that were created did not cause the rapid delamination and destruction of the sample during the test performed. The crack size comparison is shown in Table 6.

4. SUMMARY

The NbSi structure has a characteristic columnar shape. It may grow according to Thorton's rule [27]. Only the Nb-NbSi W2 sample exhibits total destruction as a result of damage to the TBC layer. It is thought that the NbSi coating on the sample showed some defects before the test. Probably the present cracks were formed during the coating process. This stands as clear evidence that even a small defect of the TBC layer may cause rapid destruction of whole composite material. In the case of sample W2, the depth of cracks could be higher than those of sample W1 and W3.

The thermal test result shows clearly that the durability of an Nb-NbSi sample is almost a binary state. The damage of TBC coating under high temperature/velocity conditions causes rapid destruction of substrate. The quality of coating surface is very important in taking care to prevent the occurrence of cracks and delamination.

The Nb-NbSi W3 sample exhibits best TBC thermal properties, with limitation of the substrate temperature to max. 1400°C. That result is understandable due to the highest Nb-Si coating thickness, which provides a more effective thermal barrier. On the other hand, a too large participation of the Si component in the TBC layer may cause the generation of brittle and low melting point phases. In the case of the Nb-NbSi W3 version of the sample, quartz and cristobalite phases were created as a result of impact of high temperature and surface local re-melting. The Si phase is highly undesirable, as it may cause cracks and excessive wear of TBC coating.

All samples that passed the test showed their ability to stabilize the temperature over time of 30 s during the thermal test. The rise time of substrate temperature takes about 10 s, after which it keeps constant values (Fig. 20).

5. CONCLUSIONS

The optimization of CVD, i.e. the pack cementation process, is needed in order to improve niobium silicides coating quality, free of cracks and other defects. To investigate what is the NbSi coating thickness influence on high temperature oxidation resistance, additional long duration thermal test are required. The depth of coating cracks should also be investigated to discover the reason for its occurrence. It may have a negative influence on oxidation resistance.

Additional XRD analysis should be prepared for specimens which have undergone thermal testing. It is needed for oxides structure identification as well as other phases.

ACKNOWLEDGEMENTS

Financial support provided by the European Space Agency, ESA Contract No. 4000122540/17/NL/CBi "High Temperature Oxidation-Proof Advanced Structures for Future Rocket Engines – HiToPaS", is hereby gratefully acknowledged.

REFERENCES

[1] S. Knittel, S. Mathieu, L. Portebois, S. Drawin, and M. Vilasi, "Development of silicide coatings to ensure the protection of Nb and silicide composites against high temperature oxidation", *Surf. Coat. Technol.*, 235, pp. 401–406, 2013, doi: 10.1016/j.surfcoat.2013.07.053.

[2] J. Cheng, S. Yi, and J. Park, "Oxidation behavior of Nb–Si–B alloys with the $NbSi_2$ coating layer formed by a pack cementation technique", *Int. J. Refract. Met. Hard Mat.*, vol. 41, pp. 103–109, 2013, doi: 10.1016/j.ijrmhm.2013.02.010.

[3] S. Cheng, S. Yi, and J. Park, "Oxidation behaviors of Nb–Si–B ternary alloys at 1100°C under ambient atmosphere", *Intermetallics*, vol. 23, pp. 12–19, 2012, doi: 10.1016/j.intermet.2011.11.007.

[4] B.P. Bewlay, M.R. Jackson, P.R. Subramanian, and J.C. Zhao, "A review of very-high-temperature Nb-silicide-based composites", *Metall. Mater. Trans. A*, vol. 34, pp. 2043–2052, 2003, doi: 10.1007/s11661-003-0269-8.

[5] R. Swadźba, "High temperature oxidation behavior of C103 alloy with boronized andsiliconized coatings during 1000h at 1100°C in air" , *Surf. Coat. Technol.*, vol. 370, pp. 331–339, 2019, doi: 10.1016/j.surfcoat.2019.04.019.

[6] J. Sun, Q.G. Fu, L.P. Guo, and L. Wang, "Silicide coating fabricated by HAPC/SAPS combination to protect niobium alloy from oxidation", *ACS Appl. Mater. Interfaces*, vol. 8, pp. 15838–15847, 2016, doi: 10.1021/acsami.6b04599.

[7] J. Sun, T. Li, G.-P. Zhang, and Q.-G. Fu, "Different oxidation protection mechanisms of HAPC silicide coating on niobium alloy over a large temperature range", *Journal of Alloys and Compounds*, vol. 790, pp. 1014–1022, 2019, doi: 10.1016/j.jallcom.2019.03.229.

[8] H.P. Martinz, B. Nigg, J. Matej, M. Sulik, H. Larcher, and A. Hoffmann, "Properties of the SIBOR® oxidation protective coating on refractory metal alloys", *Int. J. Refract. Met. Hard Mat*., vol. 24, pp. 283–291, 2006, doi: 10.1016/j.ijrmhm.2005.10.013.

[9] K. Tatemoto, Y. Ono, and R.O. Suzuki, "Silicide coating on refractory metals in molten salt", *J. Phys. Chem. Solids*, vol. 66, pp. 526–529, 2005, doi: 10.1016/j.jpcs.2004.06.043.

[10] B.V. Cockeram and R.A. Rapp, "Oxidation-resistant boron- and germanium-doped silicide coatings for refractory metals at high temperature", *Mater. Sci. Eng. A*, vol. 192–193, part 2, pp. 980–986, 1995, doi: 10.1016/0921-5093(95)03342-4.

[11] L. Zheng, E. Liu, Z. Zheng, L. Ning, J. Tong, and Z. Tan, "Preparation of alumina/aluminide coatings on molybdenum metal substrates, and protection performance evaluation utilizing a DZ40M superalloy casting test", *Surf. Coat. Technol.*, vol. 395, p. 125931, 2020, doi: 10.1016/j.surfcoat.2020.125931.

[12] M. Zielińska, M. Zagula-Yavorska, J. Sieniawski, and R. Filip, "Microstructure and oxidation resistance of an aluminide coating on the nickel based superalloymar m247 deposited by the cvd aluminizing process", *Arch. Metall. Mater.*, vol. 58, no. 3 pp. 697–701, 2013, doi: 10.2478/amm-2013-0057.

[13] Y. Garip, "Production and microstructural characterization of nb-si based in-situ composite", *Bull. Pol. Acad. Sci. Arch. Metall. Mater.*, vol. 65, no. 2 pp. 917–921, 2020, doi: 10.24425/amm.2020.132839.

[14] M. Vilasi, G. Venturini, J. Steinmetz, and B. Malaman, "Crystal structure of triniobium triiron chromium hexasilicide $Nb_3Fe_3Cr_1Si_6$: an intergrowth of $Zr_4Co_4Ge_7$ and $Nb_2Cr_4Si_5$ blocks", *J. Alloy. Compd.*, vol. 194, pp. 127–132, 1993, doi: 10.1016/0925-8388(93)90657-9.

[15] M. Vilasi, M. Francois, R. Podor, and J. Steinmetz, "New silicides for new niobium protective coatings", *J. Alloy. Compd.*, vol. 264, pp. 244–251, 1998, doi: 10.1016/S0925-8388(97)00234-X

[16] M. Vilasi, M. Francois, H. Brequel, R. Podor, G. Venturini, and J. Steinmetz, "Phase equilibria in the Nb–Fe–Cr–Si System", *J. Alloy. Compd.*, vol. 269, pp. 187–192, 1998, doi: 10.1016/S0925-8388(98)00142-X.

[17] S. Knittel, S. Mathieu, and M. Vilasi, "$Nb_4Fe_4Si_7$ coatings to protect niobium and niobium silicide composites against high temperature oxidation", *Surf. Coat. Technol.*, vol. 235, pp. 144–154, 2013, doi: 10.1016/j.surfcoat.2013.07.027.

[18] S. Majumdar, T.P. Senguptab, G.B. Kaleb, and I.G. Sharma, "Development of multilayer oxidation resistant coatings on niobium and tantalum", *Surf. Coat. Technol.*, vol. 200, pp. 3713–3718, 2006, doi: 10.1016/j.surfcoat.2005.01.034.

[19] S. Majumdar, A. Arya, I.G. Sharma, A.K. Suri, and S. Banerjee, "Deposition of aluminide and silicide based protective coatings on niobium", *App. Surf. Sci.*, vol. 257, pp. 635–640, 2010, doi: 10.1016/j.apsusc.2010.07.055.

[20] L. Portebois, S. Mathieu, Y. Bouizi, M. Vilasi, and S. Mathieu, "Effect of boron addition on the oxidation resistance of silicide protective coatings: A focus on boron location in as-coated and oxidised coated niobium alloys", *Surf. Coat. Technol.*, vol. 253, pp. 292–299, 2014, doi: 10.1016/j.surfcoat.2014.05.058.

[21] L. Xiao, X. Zhou, Y. Wang, R. Pu, G. Zhao, Z. Shen, and Y. Huang, S.Liu, Z.Cai, X.Zhao,, "Formation and oxidation behavior of Ce-modified $MoSi_2$–$NbSi_2$ coating on niobium alloy", *Corrosion Sci.*, vol. 173, p. 108751, 2020, doi: 10.1016/j.corsci.2020.108751.

[22] J. Sun, Q. Fu, and L.Guo, "Influence of siliconizing on the oxidation behavior of plasma sprayed $MoSi_2$ coating for niobium based alloy", *Intermetallics*, vol. 72, pp. 9–16, 2016, doi: 10.1016/j.intermet.2016.01.006.

[23] M. Pons, M. Caillet, and A. Galerie, "High temperature oxidation of niobium superficially coated by laser treatment", *Mater. Chem. Phys.*, vol. 15, pp. 423–432, 1987, doi: 10.1016/0254-0584(87)90062-9.

[24] B.A. Pinto, A. Sofia, and C.M. D'Oliveira, "Nb silicide coatings processed by double pack cementation: Formation mechanisms and stability", *Surf. Coat. Technol.* 409, 2021, doi: 10.1016/j.surfcoat.2021.126913.

[25] R. Swadźba *et al.*, "Characterization of Si-aluminide coating and oxide scale microstructure formed on γ-TiAl alloy during long-term oxidation at 950°C", *Intermetallics*, vol. 87, pp. 81–89, 2017, doi: 10.1016/j.intermet.2017.04.015.

[26] R. Swadźba, L. Swadźba, B. Mendala, P.-P. Bauer, N. Laska, and U. Schulz, "Microstructure and cyclic oxidation resistance of Si-aluminide coatings on γ-TiAl at 850°C", *Intermetallics*, vol. 87, pp. 81–89, 2017, doi: 10.1016/j.surfcoat.2020.126361.

[27] J.A. Thornton, "High rate thick film growth", *Ann. Rev. Mater. Sci.*, vol. 7, pp. 239–246, 1977, doi: 10.1146/annurev.ms.07.080177.001323.